Palmitoylated calnexin is a key component of the ribosome-translocon complex.

Lakkaraju, Asvin K K ; Abrami, Laurence ; Lemmin, Thomas ; Blaskovic, Sanja ; Kunz, Béatrice ; Kihara, Akio ; Dal Peraro, Matteo ; van der Goot, Françoise Gisou

Abstract: A third of the human genome encodes N-glycosylated proteins. These are co-translationally translocated into the lumen/membrane of the endoplasmic reticulum (ER) where they fold and assemble before they are transported to their final destination. Here, we show that calnexin, a major ER chaperone involved in glycoprotein folding is palmitoylated and that this modification is mediated by the ER palmitoyltransferase DHHC6. This modification leads to the preferential localization of calnexin to the perinuclear rough ER, at the expense of ER tubules. Moreover, palmitoylation mediates the association of calnexin with the ribosome-translocon complex (RTC) leading to the formation of a supercomplex that recruits the actin cytoskeleton, leading to further stabilization of the assembly. When formation of the calnexin-RTC supercomplex was affected by DHHC6 silencing, mutation of calnexin palmitoylation sites or actin depolymerization, folding of glycoproteins was impaired. Our findings thus show that calnexin is a stable component of the RTC in a manner that is exquisitely dependent on its palmitoylation status. This association is essential for the chaperone to capture its client proteins as they emerge from the translocon, acquire their N-linked glycans and initiate folding.

DOI: https://doi.org/10.1038/emboj.2012.15

Palmitoylated calnexin is a key component of the ribosome-translocon complex

Asvin K.K. Lakkaraju[1#], Laurence Abrami[1#], Thomas Lemmin [2], Sanja Blaskovic[1], Béatrice Kunz[1], Akio Kihara[3], Matteo Dal Peraro[2] and F. Gisou van der Goot[1*]

[1] *Global Health Institute*, *Ecole Polytechnique Fédérale de Lausanne (EPFL), Station 15, CH-1015 Lausanne, Switzerland*

[2] *Institute of Bioengineering*, *Ecole Polytechnique Fédérale de Lausanne (EPFL), Station 15, CH-1015 Lausanne, Switzerland*

[3] *Faculty of Pharmaceutical Sciences, Hokkaido University, Kita 12-jo, Nishi 6-chome, Kita-ku, Sapporo 060-0812, Japan*

[#] contributed equally to this work

* Corresponding author

Contact: gisou.vandergoot@epfl.ch

Character count excluding references: 53’099

ABTRACT

A third of the human genome encodes N-glycosylated proteins. These are co-translationally translocated into the lumen/membrane of the endoplasmic reticulum (ER) where they fold and assemble before they are transported to their final destination. Here we show that calnexin, a major ER chaperone involved in glycoprotein folding is palmitoylated and that this modification is mediated by the ER palmitoyltransferase DHHC6. This modification leads to the preferential localization of calnexin to the perinuclear rough ER, at the expense of ER tubules. Moreover, palmitoylation mediates the association of calnexin with the ribosome-translocon complex (RTC) leading to the formation of a supercomplex that recruits the actin cytoskeleton, leading to further stabilization of the assembly. When formation of the calnexin-RTC supercomplex was affected by DHHC6 silencing, mutation of calnexin palmitoylation sites or actin depolymerization, folding of glycoproteins was impaired. Our findings thus show that calnexin is a stable component of the RTC in a manner that is exquisitely dependent on its palmitoylation status. This association is essential for the chaperone to capture its client proteins as they emerge from the translocon, acquire their N-linked glycans and initiate folding.

INTRODUCTION

More than a third of the human genome encodes for membrane proteins or proteins secreted into the extracellular milieu. These proteins are generally synthesized with an N-terminal signal sequence that targets the translating ribosome to the endoplasmic reticulum (ER) where it docks onto the translocon (Braakman & Bulleid, 2011). The translocon is a multiprotein transmembrane complex composed of a central sec61α tetrameric pore to which associate a number of accessory proteins such as sec61ß, sec62 or the TRAP (translocon-associated protein) complex (Skach, 2007). Once the ribosome is docked onto the translocon, synthesis resumes and the nascent protein is co-translationally translocated through the sec61 channel to the lumen of the ER. As the newly synthesized protein emerges from the translocon, it is handled sequentially by a variety of enzymes, in particular leading to the addition of N-linked glycans and the formation of disulfide bonds, which together increase the solubility and stability of the protein, as well as chaperones that promote folding by preventing aggregation of intermediates.

N-glycosylation is carried out by the oligosaccharyltransferase (OST), a hetero-oligomeric complex, which associates with the ribosome-translocon complex (RTC), allowing the addition of the branched oligosaccharide co- or post-translationally (Chavan & Lennarz, 2006). To prevent aggregation or too rapid folding, which might hinder N-glycosylation (McGinnes & Morrison, 1994), the OST (Li et al, 2008) and the general chaperone BiP/Grp78 (Hammond & Helenius, 1994) maintain the polypeptide in a folding competent state.

Glycoproteins are subsequently handled by the lectin binding chaperones calnexin and calreticulin (Aebi et al, 2010). Calnexin is a type I membrane protein and calreticulin is its soluble homologue. Proteins that undergo N-glycosylation acquire *en bloc* a glucose$_3$-mannose$_9$-*N*-acetylglucosamine$_2$ oligosaccharide. Calnexin/calreticulin can only bind monoglucosylated glycans. Oligosaccharide trimming is therefore required. This occurs immediately after the oligosaccharide has been transferred to the protein, first by ER glucosidase I, which removes the first glucose, and then by glucosidase II which removes the second. The third glucose is also trimmed by glucosidase II, but its removal requires separation and repositioning of the enzyme with respect to the substrate (Deprez et al, 2005). This repositioning provides a time window during which the monoglucosylated polypeptide can interact with calnexin/calreticulin.

Glucose trimming must be rapid since calnexin was shown to bind proteins not only post-translationally but also co-translationally (Chen et al, 1995). It has been reported that upon signaling, MAP kinase and casein kinase 2 dependent phosphorylation of calnexin on Ser-563 allows its association with ribosomes (Chevet et al, 1999). We here investigated whether other mechanisms control the ability of calnexin to capture its substrates. Calnexin recently came up in four large-scale profiling studies of S-acylated proteins (Martin & Cravatt, 2009; Merrick et al, 2011; Yang et al, 2010; Yount et al, 2010). S-acylation is the addition of a fatty acid, generally C16 –palmitate– put possibly also C18–stearate– (Kordyukova et al, 2010), to cytosolic cysteine residues via a thioester bond (Linder & Deschenes, 2007). This modification is mediated by

transmembrane palmitoyltransferases harboring a conserved cytosolic DHHC domain, 23 of which are present in the human genome (Greaves & Chamberlain, 2011). In validation of these profiling studies and in agreement with a study published during the revision of this manuscript (Lynes et al, 2011), we show that calnexin can be palmitoylated on two juxtamembranous cysteines and that this modification is mediated by a single palmitoyltransferase, DHHC6, out of the 16 DHHC enzymes present in the mammalian ER. S-acylation controls the localization of calnexin within the ER network, favoring its targeting to the central ER. While being a single copy organelle, the ER is indeed compartmentalized into a variety of still poorly characterized domains that allow it to fulfill its multiple functions, which in addition to protein folding include quality control, synthesis of most cellular lipids and storage/control of intracellular calcium (Pendin et al, 2011). The most apparent, morphologically distinct, ER regions are the highly branched tubular network that extends to the cell periphery, the dense perinuclear ER, which is formed by sheet-like structures, and the nuclear membrane (Pendin et al, 2011; Puhka et al, 2007). The two latter regions composed the rough ER, where the RTC complexes reside.

We found that calnexin is a stable component of the RTC and this association relies on calnexin S-acylation. Formation of the calnexin-RTC supercomplex leads to the recruitment of the actin cytoskeleton, which further stabilizes the assembly. The here-identified acylation-dependent interaction of calnexin with the RTC complex allows it to efficiently capture nascent

glycosylated polypeptide chains, as they emerge from the translocon, and promote their folding.

RESULTS

Calnexin is palmitoylated in the ER on two juxtamembrane cysteines

Four profiling studies (Martin & Cravatt, 2009; Merrick et al, 2011; Yang et al, 2010; Yount et al, 2010) identified, with high confidence, calnexin as a S-acylated protein in mammalian cells. By immunoprecipitation of either the endogenous or tagged calnexin from ^{3}H-palmitate labeled cells, we validated these profiling studies: the protein indeed incorporated radiolabeled palmitate, which could be removed by hydroxylamine hydrochloride treatment, indicating the involvement of a thioester bond (Fig. 1A). This does not exclude that calnexin could be modified with either shorter or longer acyl chains as found for certain viral proteins (Kordyukova et al, 2010). ^{3}H-palmitate incorporation occurred on both juxtamembranous cysteines (Fig. 1B), although somewhat more efficiently on Cys-502, which is conserved in most species as well as in the testis-specific calnexin homologue, calmegin (Fig. S1).

In contrast to other lipid modifications, S-acylation is reversible (Greaves & Chamberlain, 2011). Proteins such as Ras indeed undergo dynamic (<30 min) cycles of palmitoylation-depalmitoylation, and these cycles are crucial for their function (Rocks et al, 2010). In contrast to Ras, we found that ^{3}H-palmitate turnover on calnexin is slow (Fig. 1C). As a consequence, palmitoylated calnexin must accumulate in cells and we indeed found, as described below, that at steady state the vast majority of the protein is lipid modified. Palmitoylation of calnexin mostly occurs after it has been fully synthesized, since inhibition of

protein synthesis with cycloheximide –1 hr prior to ^{3}H-palmitate labeling– only mildly affected palmitoylation (18 ± 4% decrease, Fig. 1D).

Calnexin palmitoylation is mediated by DHHC6

We next identified the palmitoyltransferase that modifies calnexin. PCR analysis revealed that all DHHC enzymes, with the exception of DHHC15, 19 and 22, are expressed in HeLa cells (Fig. S2A). RNAi duplexes were screened for their efficiency in silencing these enzymes (Table S1, Figs. S2A). Silencing of DHHC enzymes had minor effects (<25% change) on ^{3}H-palmitate incorporation into endogenous calnexin with the exception of DHHC5 and DHHC6 (Fig. 2AB). Importantly, 3 different siRNA duplexes against DHHC6 led to a similar decrease in calnexin palmitoylation (Fig. 2A) as did an shRNA construct again the non-coding region of DHHC6 (Fig. S2B). Recomplementation of shRNA treated cells with a DHHC6 expression plasmid restored calnexin palmitoylation (Fig. S2B), indicating that the observed effect is not due to an off target effect of the shRNA or RNAi duplexes.

^{3}H-palmitate incorporation experiments were also performed upon ectopic expression of calnexin-HA. Only DHHC6 silencing led to a marked decrease palmitoylation (Fig. 2C and Fig. S2C). We currently have no clear explanation as to why DHHC5 silencing affects palmitoylation of endogenous but not ectopically expressed calnexin. DHHC6 localizes to the ER (Fig. S2D and (Gorleku et al, 2011), consistent with the calnexin localization, while DHHC5 is mostly found in the Golgi apparatus (Fig. S2D). This however does not exclude its presence in

the ER. Since DHHC6 is itself palmitoylated (personal communication, (Gorleku et al, 2011), our findings raise the possibility –which will be tested in future studies– that DHHC5 palmitoylates DHHC6 or somehow regulates its function.

We next performed the reverse experiments, we monitored the effect of DHHC overexpression. An increase in palmitoylation of endogenous as well as ectopically expressed calnexin was observed upon DHHC6 overexpression but for none of the other enzymes (Fig. 2D & S2EF). Analysis of the two single cysteine calnexin mutants showed that both cysteines are modified by the same DHHC6 enzyme (Fig. S2EF). Altogether these observations show that DHHC6 modifies calnexin on both sites. Consistent with the ubiquitous expression of calnexin, we found that the DHHC6 expression is equally broad (Fig. S3A).

Since many of the experiments described in the present work involve DHHC6 silencing, we tested whether DHHC6 siRNA triggers the Unfolded Protein Response. A gene profiling analysis using Affimetrix chips revealed that while slight changes in expression were observed for GADD45 (-1.3 fold), BiP (1.32 fold), XBP1 (1.4 fold), HERP (1.5 fold), these changes are minor in comparison to what is observed upon UPR activation. Usually UPR induction leads to 4 to 27 fold increase in the expression levels of these genes at the mRNA level (Lee et al, 2003). Also we did not observe significant XBP-1 splicing.

As a side note, DHHC6 over-expression had no effect on the palmitoylation of 4 other proteins known to be S-acylated that transit through the ER: the Transferrin receptor (Alvarez et al, 1990), the Wnt co-receptor LRP6

(Abrami et al, 2008) and the two anthrax toxin receptors TEM8 and CMG2 (Abrami et al, 2006) (Fig. S3B), suggesting a certain specificity towards calnexin.

We next investigated what percentage of the calnexin population is S-acylated at steady state in HeLa cells. We previously found that glycosylphosphatidyl inositol-anchored proteins do not migrate in 2D gels unless their lipid moiety has been removed (Fivaz et al, 2000). We inferred that palmitoylation might also affect protein migration in 2D gels. Cell extracts from control and DHHC6 RNAi treated Hela cells were analyzed by 2D-PAGE followed by Western blotting against calnexin, and actin as an internal control. The analysis was performed 72 hrs after transfection with DHHC6 siRNA. This did not affect the total level of endogenous calnexin when compared to control cells, as evidenced by 1D SDS-PAGE (Fig. 2E, left panel; also seen in 2A bottom blot). As a striking validation of our strategy, DHHC6 silencing led to a 9.1±0.9 (n=4) fold increase of the calnexin signal following 2D-PAGE, while the actin signal was unaffected (Fig. 2E, right panels). The increase in calnexin staining upon DHHC6 silencing demonstrated that at least 90% of cellular calnexin is DHHC6-modified at steady state in HeLa cells. Since both sites can be modified (Fig. 1B, 2C, S2CEF), depalmitoylation is slow and must be slow on both sites (Fig. 1C), the acylated calnexin population revealed by the 2D gel analysis is most likely modified on both sites.

In Fig. 2D, we show that overexpression of DHHC6 leads to a ≈2.5 fold increase in the incorporation of ^{3}H-palmitate into calnexin. This might at first appear inconsistent with the observation that >90% of calnexin is palmitoylated. It

is however important to note that only calnexin molecules with free cysteines can incorporate ^{3}H-palmitate. Thus the bulk of cellular calnexin (>90%) is “silent” in the ^{3}H-palmitate-incorporation assay and we are monitoring the incorporation of ^{3}H-palmitate in the remaining population. The rate at which this small population of calnexin with free cysteines becomes modified depends on the abundance of the enzyme. Thus upon DHHC6 overexpression, incorporation rates increase due to an increased amount of the enzyme and so does the signal after our 2 hrs standard incorporation (Fig. 2D).

Palmitoylation is predicted to affect the conformation of calnexin

Using predictive computational methods, we next analyzed whether palmitoylation is expected to modify the structure of the transmembrane domain (TMD) and/or cytosolic tail of calnexin. Using a topology prediction algorithm (Viklund et al, 2008), we first predicted that the membrane embedded residues span from Trp-482 to Cys-502. The TMD was then modeled as an ideal α-helix based on secondary structure predictions and consistent with the UniProt annotations (P27824). We further extended the helical sequence to include residues Glu-478 through Ser-510, in order to gain information on the conformation of the cytosolic tail. The atomistic transmembrane model was inserted into a lipid membrane bilayer and refined using molecular dynamics (MD) simulations under physiological-like conditions (e.g. pH ~7, 1 atm, 298 K). Only small fluctuations of the secondary structure were observed, which support the predicted helical conformation and the match with the hydrophobic interior of

the bilayer. The helix tilted by ~30 degrees with respect to the membrane surface normal. A distortion of 30±5 degrees in the direction of the helix axis was observed at the level of Pro-494 (Fig. 3A), as expected from the helix breaking capacity of this residue (Chang et al, 1999). This proline thus breaks the rotational symmetry of the helix with respect to its main axis. The full conservation of this residue in calnexin and calmegin (Fig. S1) suggests that the TMD kink might be of functional importance.

We next included palmitate moieties at positions Cys-502 (CyP502), Cys-503 (CyP503) or both (CyP502-503). Palmitoylation did not affect the proline-induced kink and only marginally affected the helix tilt. The MD simulations however predicted a palmitoyl-dependent orientation of the cytosolic tail with respect to the helix axis (Fig. 3B). Interestingly, palmitoylation at position 503 is predicted to have a more pronounced effect on the conformation of the cytosolic tail, indicating that both sites are not equivalent and that one of the two might have a regulatory role, predictions that will be tested in the future. Combined with the asymmetric nature of the TMD, these simulations raise the interesting possibility that palmitoylation may affect the conformation of calnexin, which in turn could modify its affinity for membrane domains and/or its capacity to interact with proteins in the membrane or in the cytoplasm.

DHHC6 affects calnexin localization

Palmitoylation of membrane proteins has been proposed to modify their affinity for specific plasma membrane micro/nano domains (Charollais & Van Der Goot,

2009; Levental et al, 2010). We therefore investigated whether DHHC6 silencing would alter the distribution of calnexin. Under control conditions, immunofluorescence staining of calnexin is observed in all three major ER compartments (Fig. 4A, for additional images see S4A), resembling the staining of the soluble lumenal ER chaperone BiP and the transmembrane RTC-associated protein TRAPα (Fig. 4B, for additional images see S4A).

When silencing DHHC6, the first observation was a change in cell morphology: cells were somewhat less elongated (see Transferrin staining bottom of Fig. 4B) and the average cell footprint was ~30% larger (Fig. S5A). The nuclear staining and size was however unaltered (Fig. 4A). When viewing through confocal stacks of a lawn of cells stained for calnexin (Movie S1A vs. Movie S1B), it readily appeared that calnexin staining was lost from the nuclear envelope upon DHHC6 silencing. This was confirmed by quantifying the cells showing a nuclear envelope calnexin staining and those that did not, by eye for multiple cells over multiple experiments (Fig. 4C). It agreement, the Pearson coefficient of co-localization of calnexin with nucleoporins strongly decreased upon DHHC6 silencing (Fig. 4D, S4B). Importantly, nuclear membrane localization of calnexin was restored upon recomplementation with the DHHC6 expressing plasmid (Fig. 4C, S4B). Disappearance from the nuclear membrane was specific to calnexin, since BiP and TRAPα staining was unaffected by DHHC6 silencing (Fig. 4BEF, Fig. S4A). While disappearance from the nuclear membrane was obvious, other changes in calnexin staining, in particular in the dense and complex perinuclear ER could not be quantified in satisfactory

manner. Our interpretation of the change in calnexin distribution is that palmitoylation increases the affinity of calnexin for ER sheets, which encompasses the entire rough ER and of which the nuclear membrane is the most exacerbated form.

Palmitoylation regulates the interaction of calnexin with the RTC

The observation that DHHC6 expression favors the localization of calnexin to the rough ER prompted us to investigate whether calnexin interacts with the RTC under steady state conditions. The central translocon component sec61α, as well as the translocon associated protein TRAPα and the ribosomal subunit L12 were recovered upon immunoprecipitation of endogenous calnexin (Fig. 5A). The interaction of calnexin with sec61α and L12 was abolished upon RNAi silencing of TRAPα (Fig. 5A), indicating first that the observed interaction of calnexin with sec61α and L12 is specific, and not due to bulk co-isolation of membrane proteins in detergent/lipid micelles. Moreover the observation indicates that the TRAP complex mediates the interaction of calnexin with the RTC. Interestingly, TRAPα silencing did not affect the localization of calnexin to the nuclear membrane (Fig. S5B), showing that DHHC6-induced perinuclear calnexin localization is not due to its interaction with RTCs.

We next silenced DHHC6 by shRNA treatment for 8 days, in order to reduce the cellular pool of S-acylated calnexin. Upon long term DHHC6 silencing, co-immunoprecipitation of TRAPα, sec61α and L12 with calnexin decreased by ≈80% (Fig. 5BC & S6A). Importantly, interaction of calnexin with the RTC was

restored by transfection with DHHC6 expressing plasmid (Fig. 5BC & S6A). RTC-interaction experiments were next carried out using the single and double cysteine mutants of calnexin, the S563A mutant -where the phosphorylation site promoting ribosome association is modified (Chevet et al, 1999)–, and the P494L mutant –where the transmembrane proline (Fig. 3A) is substituted with a hydrophobic residue to remove the kink in the TM helix. It should be noted that the two latter mutations did not prevent palmitoylation (personal communication). The calnexin-RTC interaction was abolished upon mutation of Ser-563 to alanine (Fig. 5D & S6B), indicating the importance of this residue even in resting cells (Chevet et al, 1999). The RTC-interaction was also severely affected by the P494L mutation, pointing out a central role of TMD conformation for the association (Fig. 5D). Most strikingly, mutation of either S-acylation site abolished the calnexin-RTC interaction (Fig. 5D). Thus not only must calnexin be acylated to interact with the RTC, it has to be modified on both cysteines.

Actin is recruited and stabilizes the calnexin-RTC supercomplex

Stabilization of certain membrane protein complexes/clusters has been found to dependent on the actin cytoskeleton (Abrami et al, 2010). We probed whether the calnexin-RTC supercomplex interacts with actin. Actin was pulled down upon immunoprecipitation of sec61α, TRAPα as well as calnexin (Fig. 6A). The interaction between sec61α or TRAPα with actin was strongly diminished upon silencing of calnexin (Fig. 6B), indicating firstly that the interaction observed in

Fig. 6A is specific and not due to contamination by this abundant protein, and secondly that calnexin plays a crucial role in the binding of actin to the RTC.

The interaction of calnexin with actin was dependent on its palmitoylation status as indicated by the decrease in actin association upon DHHC6 silencing (Fig. 6C). Calnexin-actin interaction was restored upon transfection with the DHHC6-expressing plasmid (Fig. S6C). The importance of palmitoylation for calnexin-actin interaction was confirmed by the weak association of the single and double cysteine calnexin mutants with actin (Fig. 6D). The fact that DHHC6 silencing had a more pronounced effect than mutation of the palmitoylation sites might be due to indirect effects of unidentified ER DHHC6 targets.

Altogether the above observations raised the possibility that actin can only be recruited to calnexin-RTC supercomplex when it is fully assembled. To test this possibility, we stripped off ribosomes from the ER membrane by a 15 min puromycin treatment. Strikingly, calnexin then no longer interacted with either the translocon or actin (Fig. 6E), indicating that indeed actin can only bind to the fully assembled supercomplex. Moreover, the puromycin effect shows that calnexin is recruited to the translocon only when the ribosome has docked.

In reverse, we investigated whether actin polymerization was important for the stabilization of the supercomplex. Inhibiting actin polymerization by a short latrunculin A treatment was sufficient to decrease the interaction of calnexin with L12, TRAPα and sec61α (Fig. 6EF), while nocodazole, which disrupts microtubules, had no effect (Fig. 6EF).

Palmitoylation of calnexin promotes the folding of glycosylated proteins

Finally we investigated whether the calnexin-RTC interaction is important for the lectin chaperone function. We first analyzed the effect of silencing either calnexin, TRAPα or DHHC6 on the production –i.e. an overall read out for synthesis, folding and secretion– of total glycoproteins. Silencing of any of the three proteins led to a significant decrease in total glycoproteins as monitored by a 20 min ^{35}S Cys/Met pulse, followed by precipitation with the lectin, concavalin A (Fig. 7A & S7A). The 30% drop in detected glycoproteins is consistent with the known redundancy of the folding systems for glycoproteins (Braakman & Bulleid, 2011). As a control, we monitored the production of cytosolic, i.e. non-N-glycosylated, proteins and found that silencing of calnexin, TRAPα or DHHC6 had no effect (Fig. S7B).

Next, we analyzed the production of two specific glycoproteins: a soluble version of alkaline phosphatase (SEAP: secreted alkaline phosphatase), which provides a quantitative readout upon secretion –again used as an overall read out for synthesis, folding and secretion– (Lakkaraju et al, 2008) and the prion protein PrP, which undergoes a characteristic change in migration by SDS-PAGE upon folding and maturation (Fons et al, 2003).

DHHC6 silencing led to a 30% decrease in SEAP secretion (Fig. 7B). In contrast, secretion of the non-glycosylated protein bovine preprolactin, a well-studied protein translocation substrate (Lakkaraju et al, 2008), was not affected by DHHC6 silencing (Fig. S7C).

To assess the direct involvement of calnexin and the importance of its palmitoylation status, we silenced calnexin by shRNA and recomplemented the cells with WT or mutant calnexins (Fig. S7D). Calnexin silencing led to a 70% drop in SEAP secretion, which could be restored to >80% of control cells, upon recomplementation with the WT protein (Fig. 7C). In contrast, no recovery was observed upon recomplementation with palmitoylation-deficient calnexin (AA mutant) (Fig. 7C), while single cysteine and S563A mutants led to a very weak recovery (Fig. 7C). Altogether, these observations show that DHHC6-mediated palmitoylation of calnexin on both cysteines is required for optimal folding and secretion of SEAP.

We next monitored maturation of GFP-tagged prion protein (PrP), which upon expression in control cells migrates by SDS-PAGE predominantly in a mature form with some precursor form (Fig. 7D). Neither the mature nor the precursor PrP forms were detectable by Western blotting upon silencing of calnexin, TRAPα or DHHC6. Synthesis of PrP precursor was however unaffected by the calnexin, TRAPα or DHHC6 silencing as determined by a 5 min ^{35}S-pulse labeling of PrP (bottom of panel Fig. 7D and quantification Fig. S7E). Thus, in the absence of these proteins, PrP is rapidly degraded following synthesis. A similar rapid post-translational degradation of PrP was observed upon Latrunculin A treatment (Fig. 7E), further supporting that proper folding of PrP requires the fully assemble calnexin-RTC supercomplex.

Altogether the above experiments indicate that S-acylation controls the ability of calnexin to acts as a chaperone. To address this point specifically, we

monitored the binding of monoglucosylated substrates to calnexin. DHHC6 was silenced or not using shRNA and newly synthesized proteins were metabolically labeled. After detergent solubilizing the cells, calnexin-substrate complexes were isolated by immunoprecipitation against calnexin. As a control, cells were pretreated or not with castanospermine (CST), a specific inhibitor of α-glucosidases which prevents the generation of monoglucosylated proteins (Hammond & Helenius, 1994). Importantly castanospermine had no effect on either palmitoylation or depalmitoylation of calnexin (not shown). Also catanospermine did not alter the cellular localization of calnexin nor its interaction with the RTC (not shown).

After a pulse of metabolic labeling, a well-defined pattern of calnexin substrates was detected in control cells, which was absent in castanospermine treated cells (Fig. 7F, left panel). DHHC6 silencing led to a drastic decrease in the amount of calnexin-bound substrates, without affecting their pattern (Fig. 7F, left panel). Even when the metabolic pulse was followed by a chase period, substrate binding could not be observed in DHHC6 silenced cells, indicating that not only co- but also post-translational binding was defective. To confirm that non-acylated calnexin is unable to capture its substrates, substrate binding of the AA palmitoylation deficient mutant calnexin was monitored in comparison to WT, in cells where endogenous calnexin was silenced by shRNA. As shown in Fig. 7F (right panel), palmitoylation deficient calnexin failed to bind its substrates. This observation however does not necessarily mean that the capacity of calnexin to binding monoglucosylated proteins *per se* is affected. It reveals that in the

cellular context, calnexin must be palmitoylated and be part of the RTC complex to grab its substrates. If substrates are not captured co-translationally, they either aggregate or are handled by other folding systems in the ER, but calnexin will not bind them pots-translationally.

DISCUSSION

Calnexin is a transmembrane chaperone that aids in the folding of glycosylated proteins by binding to monoglucose residues on the branched N-linked oligosaccharide and thus protects the protein from aggregation. The interaction of calnexin with nascent chains has been observed more than 15 years ago (Chen et al, 1995), but little information was available on the specific mechanisms that may facilitate this co-translational interaction. We here report that calnexin is a stable component of the RTCs –as is the OST– leading to the formation of a supercomplex. This interaction occurs via the translocon-associated complex TRAP. Based on X-ray crystallography and single particle analysis, a model of the translocon complex has been proposed wherein TRAPα interacts with sec61α, the latter interacting via the opposing face of the molecule with sec61ß (Menetret et al, 2008). Our findings thus allow a rough positioning of calnexin in this supercomplex, sandwiching TRAPα between calnexin and the translocon (Fig. 8).

Formation and stabilization of calnexin-RTC supercomplex requires several factors. As previously described (Chevet et al, 2010), Ser-563 is critical possibly due to its phosphorylation. The kinked conformation of the transmembrane domain also influences the interaction, as indicated by the disruptive effect of mutating the highly conserved TM Pro-494. Importantly, calnexin must be palmitoylated.

Despite the presence of 12 (Ohno et al, 2006) to 16 (our unpublished observations in Hela cells) palmitoyltransferase in the mammalian ER, the S-

acylation of calnexin is performed by a single enzyme, DHHC6. The involvement of a single DHHC enzyme was rather unexpected since these enzymes are thought to have broad overlapping specificities at least for soluble substrates (Greaves & Chamberlain, 2011). Also in contrast to soluble substrates such as Ras, calnexin does not undergo dynamic cycles of palmitoylation-depalmitoylation. As a consequence, at steady state, the S-acylated form –and most likely the dual acylated form– accumulates and almost the entire pool of cellular calnexin is modified in resting cells as shown by our 2D gel analysis. The observed slow rate of palmitate turnover might be due to the close proximity, and possibly even embedding, of the cysteine residues in the membrane, which would render them inaccessible to cytosolic thioesterases, of which only one has so far been identified, the soluble enzyme APT1 (Dekker et al, 2010). Recently it has been observed for ß1-adrenergic receptor that the susceptibility of cysteines to thioesterases indeed correlates with distance from the transmembrane domain (Zuckerman et al, 2011).

S-Acylation of calnexin promotes its interaction with the RTC in two ways: Firstly, palmitoylation affects the ability of calnexin to interact with the TRAP complex, possibly by influencing the conformation of the TMD and/or the cytosolic tail as suggested by the MD simulations. Secondly, palmitoylation favors the association of calnexin with the nuclear membrane, and probably with sheet-like ER structures in general. Calnexin spans the membrane only once and it is therefore unlikely that it has any membrane curvature sensing capacity. Since protein and lipid compositions are likely different in ER tubules vs. ER

sheets (Shibata et al, 2010; Shibata et al, 2008), palmitoylation may favor the partitioning of calnexin to sheet-like structures, in a manner similar to raft-partitioning of transmembrane proteins at the plasma membrane (Levental et al, 2010). Calnexin has also been shown to localize to Mitochondrial Associated Membranes (MAM), sites of interaction between the ER and mitochondria (de Brito & Scorrano, 2010; Myhill et al, 2008). During the revision of this manuscript, localization of calnexin as well as of TMX, a transmembrane ER-thioredoxin, to MAMs was reported to depend on palmitoylation of these two type I membrane proteins (Lynes et al, 2011). Future studies should elucidate whether and how S-acylation dependent localization of calnexin to the various ER domains is controlled.

Interestingly, once fully assembled, the calnexin-RTC supercomplex recruits the actin cytoskeleton, which in turn is required to stabilize the assembly. While in yeast and plants where cortical ER is known to move along actin cables (Du et al, 2004), few reports describe interactions between actin and the ER in animal cells (Du et al, 2004). Actin is well known to interact with the nuclear envelope via Nesprins, large transmembrane proteins involved in nuclear positioning and nuclear-envelope architecture (Lombardi et al, 2011). However interactions with the rest of the ER have not been reported with the exception of a study showing that actin controls the diffusion of newly synthesized glycoproteins in the ER lumen and thereby reduces aggregation during folding (Nagaya et al, 2008). Our observations raise the possibility that this is due to the handling of these glycoproteins by the calnexin-RTC supercomplexes.

Altogether the present work leads to a model where DHHC6-mediated S-acylation favors the partitioning of calnexin into the rough ER and, in addition, allows it to interact with RTC components leading to the formation of a supercomplex, which subsequently recruits the actin cytoskeleton, the polymerization of which in turn is required to maintain the assembly (Fig. 8). When the nascent polypeptide chain emerges from the translocon pore, it arrives into a folding prone microenvironment: the OST and BiP initially keep it in an unfolded state to allow optimal N-glycosylation and also await the full synthesis of folding units. By being an integral part of the ribosome-translocon supercomplex, calnexin is ideally positioned to capture its client protein following appropriate glucose trimming, protecting the protein from aggregation as it undergoes oxidative folding, further benefiting from the calnexin-associated oxidoreductase ERp57.

MATERIALS AND METHODS

Cell culture, plasmids, transfections and real time-PCR

HeLa cells (ATCC) were grown in complete Modified eagles medium (MEM) (Sigma) at 37°C supplemented with 10% fetal bovine serum (FBS), 2 mM L-glutamine, penicillin and streptomycin. RPE1 cells were grown in complete Dulbeccos MEM (DMEM) (Gibco) supplemented with 10% fetal bovine serum (FBS), 2 mM L-glutamine, penicillin and streptomycin. Mammalian expression plasmids harboring human C-terminally tagged Calnexin-HA and Calnexin-GFP were generated by cloning the calnexin cDNA into pCDNA3 vector bearing the HA tag or GFP. Constructs to express single or double point mutation of calnexin were generated using the Quickchange (Stratagene) strategy following manufacturer instructions. Isoform 1 of human tumor endothelial marker 8 (TEM8) cDNA tagged with a HA epitope was cloned in the pIREShyg2 vector. Plasmid encoding human myc-LRP6 was provided by Dr. G. Davidson. GFP-PrP was provided by Dr. Chiara Zurzolo. PPL-3f was provided by Dr. Katharina Strub. Human DHHC cDNA were cloned in pCE puro-His-myc or flag expressing plasmids. Plasmids were transfected into cells for 24 or 48 hrs (2 µg cDNA/9.6 cm^2 plate) using Fugene (Roche Diagnostics Corporation). For control transfections, we used an empty pCDNA3 plasmid. shRNA against calnexin were generated from the p.Super.Retro.Puro vector containing the hairpin insert against the following target sequence present at the 3' UTR of calnexin gene: 5'-gagcttgatctgtgatttc- 3'(Table S1). As a control, we used shRNA against the target sequence in firefly luciferase gene: 5′-CGTACGCGGAATACTTCGA-3′. shRNA

against DHHC6 was generated by cloning the hairpin insert against the target region in the 3´UTR of DHHC6: 5'CCTAGTGCCATGATTTAAA3' (Table S1).

For the real-time PCR, RNA was extracted from a 6 well dish using the RNeasy kit (Qiagen). 1 mg of the total RNA extracted was used for the reverse transcription using random hexamers and superscript II (Invitrogen). A 1:40 dilution of the cDNA was used to perform the real-time PCR using SyBr green reagent (Roche). mRNA levels were normalized using three housekeeping genes: TATA-binding protein (TBP), β-microglobulin and β-glucoronidase (GUS). Total RNA of different human tissues was obtained from Amsbio.

Antibodies and Reagents

Polyclonal antibodies against calnexin were generated against the C-terminal peptide: CDAEEDGGTVSQEEEDRKPK in rabbit; rat antibodies against purified CMG2 were produced in our laboratory; anti-HA and anti-GFP were from Roche; Anti-flag M2 antibody from Sigma; anti-HA-agarose conjugated beads, used for the immunoprecipitations from Roche (Applied Science, IN); anti-calnexin monoclonal and anti-myc antibodies from Santa Cruz; anti-actin antibodies from Millipore; anti-transferrin receptor antibodies from Zymed; anti-Nuclear Pore Complex Proteins (Mab414), anti-Sec61α, anti-BiP antibodies from Abcam. Anti-L12 antibodies were provided Dr. K. Strub. Anti-TRAPα antibody was provided by Dr. R. Hegde. Protein G-agarose conjugated beads were from GE Healthcare, HRP secondary antibodies were from Pierce, and Alexa-conjugated secondary antibodies from Molecular Probes. Latrunculin A (used at a concentration of

0.4mg/ml for 30 min or 1h) and Nocodazole (used at a concentration of 10μM for 30 min or 1h) were from Sigma. Castanospermine was purchased from Calbiochem and used at a concentration of 1mM. Puromycin was purchased from Calbiochem and used at a concentration of 200μM for 15 min to strip the ER of ribosomes in HeLa cells.

Immunoprecipitation and RNAi experiments

siRNA against human DHHC were purchased from Qiagen (see Table S1). As control siRNA we used the following target sequence of the viral glycoprotein VSV-G: 5'attgaacaaacgaaacaagga 3'. For gene silencing, Hela cells were transfected for 72 hrs with 100 pmol / 9.2 cm2 dish of siRNA using interferrin (Polyplus) transfection reagent.

For all immunoprecipitations unless specified, cells were lysed 30 min at 4°C in IP buffer (0.5%NP40, 500 mM Tris-HCl pH 7.4, 20 mM EDTA, 10 mM NaF, 2 mM benzamidine, and a cocktail of protease inhibitors, Roche) followed by centrifugation for 3 min at 2000 g. The supernatants were precleared with protein G-agarose conjugated beads and incubated 16 h at 4°C with antibodies and beads. The beads were washed for three times with the IP buffer and resuspended in the sample buffer (2x) after the final wash. The samples were heated at 95°C for 5 min and migrated on SDS-PAGE. Western blotting was performed using the iBlot (Invitrogen) according to the manufacturers instructions. Quantification of the blots was done either using the typhoon imager or Image J software.

Radiolabeling experiments

To monitor palmitoylation, HeLa cells transfected with either the wild type or mutant calnexin constructs were incubated for 2hrs at 37°C in IM (Glasgow minimal essential medium buffered with 10 mM Hepes, pH 7.4) with 200 µCi /ml ^{3}H palmitic acid (9,10-^{3}H(N)) (American Radiolabeled Chemicals, Inc). The cells were washed and the cell lysate was extracted followed by immunoprecipitation with tag specific antibodies in the case of exogenously expressed calnexin and calnexin antibody in case of endogenous protein. After the washes, beads were incubated for 5 min at 90°C in non-reducing sample buffer (2x) prior to SDS-PAGE. After the SDS-PAGE, the gel was incubated with a fixative solution (25% isopropanol, 65% H_2O, 10% acetic acid), followed by a 30 min incubation with signal enhancer Amplify NAMP100 (Amersham). The dried gels were exposed to a Hyperfilm MP (Amersham). Chemical removal of S-palmitoylation was performed by treating cell extracts for 1h at room temperature with 1M hydroxylamine hydrochloride (Sigma) pH 7.2. Protein synthesis was blocked by 1hr treatment with 10 µg/ml cycloheximide (Sigma) at 37°C.

To monitor the ability of calnexin to bind substrates, HeLa cells were first transfected with the shRNA against calnexin for 7 to 9 days. After 96hrs, cells were retransfected with either the wild type or the AA mutant calnexin for 48 hrs.

Cells were pretreated or not for 1h with 1mM castanospermine (CST), a specific inhibitor of α-glucosidases and pulse labeled with 100µCi/ml ^{35}S-methionine/cysteine for 10 min followed by a 3 min chase in the presence or

absence of drug. Cells were harvested in an isotonic HEPES buffer (pH-6.8) containing 2%CHAPS and protease inhibitor cocktail. Post nuclear supernatants, obtained by centrifuging the sample at 10000g for 10 min, were submitted to immunoprecipitation overnight with anti-calnexin antibody followed by incubation with protein G agarose beads for 2hrs at 4°C.

To monitor the synthesis and maturation of GFP-PrP protein, HeLa cells transfected with GFP-PrP under different experimental conditions were labeled with 100µCi/ml ^{35}S-methionine/cysteine for 30 min. The cells were then lysed in lysis buffer composed of 0.1M Tris-HCl pH-8 and 1% SDS. The cell lysate was heated at 95°C for 10 min with occasional stirring until the lysate is no more viscous. The cleared lysate was diluted in the RIPA buffer (150 mM NaCl, 1% NP-40, 0.5% deoxycholate, 0.1% SDS, 50 mM Tris-HCl [pH 8], 1 mM EDTA, and 1X protease inhibitor cocktail). Immunoprecipitation was performed using an anti-GFP antibody.

For all the experiments, samples were analyzed by 4-12% gradient SDS-PAGE, followed by fixing and drying of the gels. The radiolabeled products were revealed using Typhoon phosphoimager and the quantified using the Typhoon Imager (Image QuantTool, GE healthcare).

Glycoprotein analysis

Fractionation of newly synthesized glycoproteins was performed in 35mm dishes. Cells were metabolically labeled with 50 µCi/ml of ^{35}S- Methionine / cysteine mix for 20 min, followed by a wash with ice-cold PBS. Cytosolic proteins were

extracted by treating the cells with 150µg/ml of digitonin in KHM buffer (110 mM KAc, 20 mM Hepes, pH 7.2, 2 mM MgAc2) for 5min. After the recovery of cytosolic extract, the cells were washed once again in the KHM buffer and resuspended in 500 µl of the IP buffer to extract the non-cytosolic proteins. The glycoproteins were separated from the non-cytosolic protein fraction by incubation with Con-A beads (GE Healthcare) for 1hr. Equal amounts of total protein were loaded on the Con-A beads from all the samples Con-A beads selectively bind to the glycoproteins. The beads were washed for three times with the IP buffer and the glycoproteins were eluted by 300 µl of IP buffer containing 0.25 M α-methyl- D-mannopyranoside. Both the cytosolic and glycoprotein fractions were migrated on 4-20% SDS PAGE gradient gels. The gels were fixed, dried and further analyzed for autoradiography.

Calnexin complementation and SEAP Assay

For the complementation assay, HeLa cells were transfected with shRNA against calnexin and the transfected cells were selected by treating with puromycin (3µg/ml) for 24h. At 72h post transfection the cells were split into 6 well plates and the day after were transfected with the control plasmid, the wild type or the mutant calnexin cDNAs and when required with the pSEAP2 reporter plasmid.

SEAP assay was performed using Great EscAPe SEAP Chemiluminescence Kit 2.0 (Clonetech). The cell medium was changed 24h before the SEAP assay was done in order to monitor the SEAP secreted for 24h when the RNAi or the over expression is most effective. Assay was performed in a 96 well plate, using 15µl

of the growth medium according to the manufacturers instructions. The Chemiluminescence signal was collected by Spectra Max multiwell plate reader and the data was analyzed by Soft Max Pro 5 software.

DHHC6 recomplementation

For the complementation assay HeLa cells were transfected with shRNA against DHHC6 followed by selection of transfected cells by treating with puromycin (3µg/ml) for 24h. The cells were further transfected on day6 with the cDNA expressing human DHHC6 without its 3´UTR for complementation. The functional assays were performed on day 8 to analyze the restoration of phenotypes observed by the loss of DHHC6.

Immunofluorescence microscopy

Immunofluorescence in HeLa was done as described previously with the exception of the fixative used. To label the plasma membrane of the cells, the cells were treated with 5µg/ml of FITC labeled Transferrin (Molecular probes) for 1h at 4°C. This was followed by washes at 4°C and fixation. Cells were fixed and permeabilized with methanol at -20°C for 4 min. Cells were further labeled with the appropriate primary antibody, followed by labeling with Alexa-conjugated goat anti-rabbit or anti-mouse IgG (405nm, 488nm, 568nm). The nuclei were stained by Hoechst dye. Images were acquired using a 63x lens on LSM-710 Laser scanning microscope (Carl Zeiss Microimaging, Inc.). The Zen software was used for the processing of the images and the 3D stacks. The movie animations

and the summation of the z-stacks were done using the Image J software. To calculate the Pearson correlation coefficient, four different regions on the nuclear membrane were analyzed for 15 cells. Each condition was subjected to a total of 60 regions and the Pearson coefficient was calculated using Coloc 2 plugin in FIJI software.

Molecular dynamics simulations

We used molecular dynamics (MD) simulations to characterize the calnexin TM domain at the atomistic level in the membrane environment. As a first step, the ideal helical TM model was inserted and equilibrated in a 60x60 $Å^2$ Palmitoyl Oleoly Phosphatidyl Choline (POPC) membrane patch (Humphrey et al, 1996) to characterize its structure and dynamics in a phospholipid bilayer. A Palmitoyl group was then covalently linked to C502 and C503 sulfur atoms to form the single and double palmitoylated calnexin models.

All simulations were performed using the NAMD (Phillips et al, 2005) engine, in combination with the CHARMM27 force field brooks, including CMAP corrections. TIP3P water (Jorgensen et al, 1983) parameterization was used to describe the water molecules. The spatial overlapping of lipid molecules and protein were removed and the resulting protein-membrane system was solvated in variable-size water box, at a salt concentration of 150 mM NaCl. The periodic electrostatic interactions were computed using the particle-mesh Ewald (PME) summation with a grid spacing smaller then 1 Å. All systems were first minimized by 2000 conjugate gradient steps, and subsequently gradually heated from 0 to

300 K in 800 ps with a constraint on the protein backbone scaffold. Finally, the systems were equilibrated for 10 ns at 300K. Free molecular dynamics of all equilibrated system were run for not less than 50 ns with a 2 fs integration time step using the RATTLE algorithm applied to all bonds, and trajectories collected for analysis. Constant temperature (300K) was imposed by using Langevin dynamics (Brunger & Brooks, 1984), with damping coefficient of 1.0 ps. Constant pressure of 1 atm was maintained with a Langevin piston dynamics (Feller et al, 1995) 200 fs decay period and 50 fs time constant.

Statistical analysis

All experiments were performed at least 3 times, independently. Two-tailed T-tests were performed to evaluate the significance of the data.

ACKNOWLEDGEMENTS

We thank L. Symul for the graphics work in Fig. 8, G. Davidson for the myc-LRP6 plasmid, C. Zurzolo for the PrP plasmid, K. Strub for the PPL-3f plasmid and anti-L12 antibodies, R. Hedge for anti-TRAPα antibodies. This work was supported by the Swiss National Science Foundation and the EuroMembrane in the context of the EUROCORES program from the European Science Foundation.

AUTHORS CONTRIBUTIONS AND CONFLICTS OF INTEREST

AL, LA conceived and performed experiments, analyzed the data and wrote the manuscript. TL and MDP performed the molecular dynamics experiments and critically read the manuscript. SB and BK performed experiments, AK provide the DHHC expressing plasmids. GVDG conceived experiments, analyzed the data and wrote the manuscript.

All authors declare that there is no conflict of interest.

REFERENCES

Abrami L, Bischofberger M, Kunz B, Groux R, van der Goot FG (2010) Endocytosis of the anthrax toxin is mediated by clathrin, actin and unconventional adaptors. *PLoS Pathog* **6:** e1000792

Abrami L, Kunz B, Iacovache I, van der Goot FG (2008) Palmitoylation and ubiquitination regulate exit of the Wnt signaling protein LRP6 from the endoplasmic reticulum. *Proc Natl Acad Sci U S A* **105:** 5384-5389

Abrami L, Leppla SH, van der Goot FG (2006) Receptor palmitoylation and ubiquitination regulate anthrax toxin endocytosis. *J Cell Biol* **172:** 309-320

Aebi M, Bernasconi R, Clerc S, Molinari M (2010) N-glycan structures: recognition and processing in the ER. *Trends in biochemical sciences* **35:** 74-82

Alvarez E, Girones N, Davis RJ (1990) A point mutation in the cytoplasmic domain of the transferrin receptor inhibits endocytosis. *Biochem J* **267:** 31-35

Braakman I, Bulleid NJ (2011) Protein Folding and Modification in the Mammalian Endoplasmic Reticulum. *Annu Rev Biochem* **80:** 71-99

Brunger A, Brooks CL (1984) Stochastic boundary conditions for molecular dynamics simulations of ST2 water. *Chemical Physics Letters* **105:** 495-500

Chang DK, Cheng SF, Trivedi VD, Lin KL (1999) Proline affects oligomerization of a coiled coil by inducing a kink in a long helix. *J Struct Biol* **128:** 270-279

Charollais J, Van Der Goot FG (2009) Palmitoylation of membrane proteins (Review). *Mol Membr Biol* **26:** 55-66

Chavan M, Lennarz W (2006) The molecular basis of coupling of translocation and N-glycosylation. *Trends Biochem Sci* **31:** 17-20

Chen W, Helenius J, Braakman I, Helenius A (1995) Cotranslational folding and calnexin binding during glycoprotein synthesis. *Proc Natl Acad Sci U S A* **92:** 6229-6233

Chevet E, Smirle J, Cameron PH, Thomas DY, Bergeron JJ (2010) Calnexin phosphorylation: linking cytoplasmic signalling to endoplasmic reticulum lumenal functions. *Semin Cell Dev Biol* **21:** 486-490

Chevet E, Wong HN, Gerber D, Cochet C, Fazel A, Cameron PH, Gushue JN, Thomas DY, Bergeron JJ (1999) Phosphorylation by CK2 and MAPK enhances calnexin association with ribosomes. *EMBO J* **18:** 3655-3666

de Brito OM, Scorrano L (2010) An intimate liaison: spatial organization of the endoplasmic reticulum-mitochondria relationship. *The EMBO journal* **29:** 2715-2723

Dekker FJ, Rocks O, Vartak N, Menninger S, Hedberg C, Balamurugan R, Wetzel S, Renner S, Gerauer M, Scholermann B, Rusch M, Kramer JW, Rauh D, Coates GW, Brunsveld L, Bastiaens PI, Waldmann H (2010) Small-molecule inhibition of APT1 affects Ras localization and signaling. *Nat Chem Biol* **6:** 449-456

Deprez P, Gautschi M, Helenius A (2005) More than one glycan is needed for ER glucosidase II to allow entry of glycoproteins into the calnexin/calreticulin cycle. *Molecular cell* **19:** 183-195

Du Y, Ferro-Novick S, Novick P (2004) Dynamics and inheritance of the endoplasmic reticulum. *Journal of cell science* **117:** 2871-2878

Feller SE, Zhang Y, Pastor RW, Brooks BR (1995) Constant pressure molecular dynamics simulation: the Langevin piston method. *The Journal of Chemical Physics* **103:** 4613

Fivaz M, Vilbois F, Pasquali C, van der Goot FG (2000) Analysis of GPI-anchored proteins by two-dimensional gel electrophoresis. *Electrophoresis* **21:** 3351-3356

Fons RD, Bogert BA, Hegde RS (2003) Substrate-specific function of the translocon-associated protein complex during translocation across the ER membrane. *J Cell Biol* **160:** 529-539

Gorleku OA, Barns AM, Prescott GR, Greaves J, Chamberlain LH (2011) Endoplasmic reticulum localization of DHHC palmitoyl transferases mediated by lysine-based sorting signals. *The Journal of Biological Chemistry* **286:** 39573-39584

Greaves J, Chamberlain LH (2011) DHHC palmitoyl transferases: substrate interactions and (patho)physiology. *Trends Biochem Sci* **36:** 245-253

Hammond C, Helenius A (1994) Folding of VSV G protein: sequential interaction with BiP and calnexin. *Science* **266:** 456-458

Humphrey W, Dalke A, Schulten K (1996) VMD: visual molecular dynamics. *J Mol Graph* **14:** 33-38, 27-38

Jorgensen WL, Chandrasekhar J, Madura JD, Impey RW, Klein ML (1983) Comparison of simple potential functions for simulating liquid water. *The Journal of Chemical Physics* **79:** 926

Kordyukova LV, Serebryakova MV, Baratova LA, Veit M (2010) Site-specific attachment of palmitate or stearate to cytoplasmic versus transmembrane cysteines is a common feature of viral spike proteins. *Virology* **398:** 49-56

Lakkaraju AK, Mary C, Scherrer A, Johnson AE, Strub K (2008) SRP keeps polypeptides translocation-competent by slowing translation to match limiting ER-targeting sites. *Cell* **133:** 440-451

Lee AH, Iwakoshi NN, Glimcher LH (2003) XBP-1 regulates a subset of endoplasmic reticulum resident chaperone genes in the unfolded protein response. *Molecular and cellular biology* **23:** 7448-7459

Levental I, Lingwood D, Grzybek M, Coskun U, Simons K (2010) Palmitoylation regulates raft affinity for the majority of integral raft proteins. *Proc Natl Acad Sci U S A* **107:** 22050-22054

Li H, Chavan M, Schindelin H, Lennarz WJ (2008) Structure of the oligosaccharyl transferase complex at 12 A resolution. *Structure* **16:** 432-440

Linder ME, Deschenes RJ (2007) Palmitoylation: policing protein stability and traffic. *Nat Rev Mol Cell Biol* **8:** 74-84

Lombardi ML, Jaalouk DE, Shanahan CM, Burke B, Roux KJ, Lammerding J (2011) The interaction between nesprins and sun proteins at the nuclear envelope is critical for force transmission between the nucleus and cytoskeleton. *J Biol Chem* **286:** 26743-26753

Lynes EM, Bui M, Yap MC, Benson MD, Schneider B, Ellgaard L, Berthiaume LG, Simmen T (2011) Palmitoylated TMX and calnexin target to the mitochondria-associated membrane. *The EMBO journal***:** doi: 10.1038/emboj.2011.1384.

Martin BR, Cravatt BF (2009) Large-scale profiling of protein palmitoylation in mammalian cells. *Nat Methods* **6:** 135-138

McGinnes LW, Morrison TG (1994) The role of the individual cysteine residues in the formation of the mature, antigenic HN protein of Newcastle disease virus. *Virology* **200:** 470-483

Menetret JF, Hegde RS, Aguiar M, Gygi SP, Park E, Rapoport TA, Akey CW (2008) Single copies of Sec61 and TRAP associate with a nontranslating mammalian ribosome. *Structure* **16:** 1126-1137

Merrick BA, Dhungana S, Williams JG, Aloor JJ, Peddada S, Tomer KB, Fessler MB (2011) Proteomic profiling of S-acylated macrophage proteins identifies a role for palmitoylation in mitochondrial targeting of phospholipid scramblase 3. *Molecular & cellular proteomics : MCP* **10:** M110.006007

Myhill N, Lynes EM, Nanji JA, Blagoveshchenskaya AD, Fei H, Carmine Simmen K, Cooper TJ, Thomas G, Simmen T (2008) The subcellular distribution of calnexin is mediated by PACS-2. *Molecular biology of the cell* **19:** 2777-2788

Nagaya H, Tamura T, Higa-Nishiyama A, Ohashi K, Takeuchi M, Hashimoto H, Hatsuzawa K, Kinjo M, Okada T, Wada I (2008) Regulated motion of glycoproteins revealed by direct visualization of a single cargo in the endoplasmic reticulum. *J Cell Biol* **180:** 129-143

Ohno Y, Kihara A, Sano T, Igarashi Y (2006) Intracellular localization and tissue-specific distribution of human and yeast DHHC cysteine-rich domain-containing proteins. *Biochim Biophys Acta* **1761:** 474-483

Pendin D, McNew JA, Daga A (2011) Balancing ER dynamics: shaping, bending, severing, and mending membranes. *Curr Opin Cell Biol* **4:** 435-442

Phillips JC, Braun R, Wang W, Gumbart J, Tajkhorshid E, Villa E, Chipot C, Skeel RD, Kale L, Schulten K (2005) Scalable molecular dynamics with NAMD. *J Comput Chem* **26:** 1781-1802

Puhka M, Vihinen H, Joensuu M, Jokitalo E (2007) Endoplasmic reticulum remains continuous and undergoes sheet-to-tubule transformation during cell division in mammalian cells. *J Cell Biol* **179:** 895-909

Rocks O, Gerauer M, Vartak N, Koch S, Huang ZP, Pechlivanis M, Kuhlmann J, Brunsveld L, Chandra A, Ellinger B, Waldmann H, Bastiaens PI (2010) The palmitoylation machinery is a spatially organizing system for peripheral membrane proteins. *Cell* **141:** 458-471

Shibata Y, Shemesh T, Prinz WA, Palazzo AF, Kozlov MM, Rapoport TA (2010) Mechanisms determining the morphology of the peripheral ER. *Cell* **143:** 774-788

Shibata Y, Voss C, Rist JM, Hu J, Rapoport TA, Prinz WA, Voeltz GK (2008) The reticulon and DP1/Yop1p proteins form immobile oligomers in the tubular endoplasmic reticulum. *J Biol Chem* **283:** 18892-18904

Skach WR (2007) The expanding role of the ER translocon in membrane protein folding. *J Cell Biol* **179:** 1333-1335

Viklund H, Bernsel A, Skwark M, Elofsson A (2008) SPOCTOPUS: a combined predictor of signal peptides and membrane protein topology. *Bioinformatics* **24:** 2928-2929

Yang W, Di Vizio D, Kirchner M, Steen H, Freeman MR (2010) Proteome scale characterization of human S-acylated proteins in lipid raft-enriched and non-raft membranes. *Mol Cell Proteomics* **9:** 54-70

Yount JS, Moltedo B, Yang YY, Charron G, Moran TM, Lopez CB, Hang HC (2010) Palmitoylome profiling reveals S-palmitoylation-dependent antiviral activity of IFITM3. *Nat Chem Biol* **6:** 610-614

Zuckerman DM, Hicks SW, Charron G, Hang HC, Machamer CE (2011) Differential regulation of two palmitoylation sites in the cytoplasmic tail of the {beta}1-adrenergic receptor. *J Biol Chem* **286:** 19014-19023

FIGURE LEGENDS

Figure 1: Calnexin is palmitoylated in the ER

A: HeLa cells were transfected or not (endogenous) for 48h with Calnexin-WT-GFP or Calnexin-AA-GFP. Cells were incubated with ^{3}H-palmitic acid for 2h. Cell extracts were treated or not with 1M hydroxylamine hydrochloride pH 7.2 (1h at room temperature) prior to immunoprecipitation using anti-calnexin or anti-GFP antibodies. Immunoprecipitates were split into two, run on SDS-PAGE and analyzed by autoradiography or Western blotting.

B: HeLa cells were transfected 24hrs with Calnexin-WT-HA or Calnexin-CA-HA, Calnexin-AC-HA or Calnexin-AA-HA, labeled with ^{3}H-palmitic acid and analyzed as in A by autoradiography or Western blotting (anti-HA). See Figure S1 for positions of the cysteines. Bottom panel: autoradiograms were quantified using the Typhoon Imager. Errors correspond to standard deviations (n=5).

C: Non-transfected HeLa cells were labeled as in A. The cells were then washed and incubated in the normal medium and cell lysis was performed at different time points followed by immunoprecipitation as described in A. Samples were analyzed by autoradiography and the quantification was performed using the Typhoon imager (n=3).

D: HeLa cells were pretreated or not with cycloheximide (CHX) for 1 hr followed by ^{3}H-palmitic acid labeling in the presence or absence of the drug. Immunoprecipitation was preformed using anti-calnexin antibodies Samples were analyzed by autoradiography and Western blotting (anti-calnexin). Quantification

was performed using the Typhoon Imager. Errors correspond to standard deviations (n=3).

Figure 2: Calnexin is palmitoylated by DHHC6

A: HeLa cells were transfected for 72hrs with different DHHC siRNA or control siRNA (Ctrl). Cells were incubated with ^{3}H-palmitic acid for 2h prior to immunoprecipitation using anti-calnexin antibodies. Immunoprecipitates were split into two, run on SDS-PAGE and analyzed either by autoradiography (3H-palmitate) or Western blotting (anti-calnexin).

B: Autoradiograms and western blots from (A) were quantified using the Typhoon Imager. Errors correspond to standard deviations (n=4). ** $p < 0.01$. For the identity of the siRNAs see Table S1, for their efficiency see Fig. S2A

C: HeLa cells were transfected 72hrs with Calnexin-WT-HA or Calnexin-CA-HA, or Calnexin-AC-HA and DHHC siRNAs, labeled with ^{3}H-palmitic acid. Immunoprecipitates using anti-HA antibodies were split into two, run on SDS-PAGE gels and analyzed either by autoradiography or Western blotting (see Fig. S2C). Autoradiograms and western blotting were quantified using the Typhoon Imager. Errors correspond to standard deviations (n=4).

D: HeLa cells were transfected 24hrs with human DHHC cDNA, labeled with ^{3}H-palmitic acid. Immunoprecipitates using anti-Calnexin antibodies were analyzed and quantified as in B (n=4). For analysis of cysteine mutants see Fig. S2EF.

E: HeLa cells were transfected for 72hrs with DHHC6 siRNA or control siRNA (Ctrl). Left panel: cells were labeled with ^{3}H-palmitic acid as analyzed as in A.

Right panel: 50 µg of cell extracts were analyzed using 2D-gel ZOOM IPGRunner system (Invitrogen) followed by Western blotting using anti-calnexin and anti-actin antibodies.

Figure 3: Modeling of the effect of palmitoylation on calnexin conformation

A: The atomistic models of the helical transmembrane domain of calnexin were equilibrated in a solvated DOPC membrane bilayer using molecular dynamics simulations. Cys502, Cys503 and Pro494 are shown in licorice representation. The approximate position of the membrane bilayer is shown by dashed lines.

B: Palmitoylation affects the orientation of the cytosolic tail of calnexin with respect to the axis of the transmembrane helix.

Figure 4: Effect of DHHC6 silencing on calnexin localization

A: HeLa cells were transfected with either a control shRNA or shRNA against DHHC6 for 8 days, fixed in methanol and stained with anti-calnexin and anti-nucleoporin antibodies. Bar: 10 µm.

B: HeLa cells grown on cover slips were transfected for 72h with either control siRNA or siRNA against DHHC6 and were incubated or not with fluorescent Transferrin, washed, fixed in methanol and immunostained with any one of the following antibodies: calnexin, BiP, TRAPα. Each image represents the sum of all the stacks taken in z-axis. To visualize more cells see Fig. S4A. Bar: 10 µm.

C: HeLa cells were transfected with either a control shRNA or shRNA targeting DHHC6 for 8 days. On day 6 the cells were transfected either with an empty

vector or human DHHC6 cDNA bearing a myc tag for complementation. The cells were fixed and stained with anti-calnexin, anti-nucleoporin and Hoechst dye. The cells were analyzed manually for presence or absence or restoration of the nuclear membrane staining of calnexin. 50 cells were analyzed per condition per experiment. Error bars represent the standard deviation (n=3).

D: The cells from A were imaged and the Pearson correlation coefficient for colocalization between calnexin and nucleoporins was determined by monitoring 15 cells/experiment from each condition (n=3).

E,F: Confocal stacks of cells treated as in B were analyzed manually and the number of cells showing nuclear or no nuclear membrane staining for calnexin (C), BiP (D) or TRAPα was determined. Three independent experiments were analyzed and 50 cells were counted for each experiment. Error bars represent standard deviations.

Figure 5: Palmitoylation regulates the interaction of Calnexin with the RTC.

A: HeLa cells were transfected for 72h with either the control siRNA or a siRNA against TRAPα. Immunoprecipitates against anti-calnexin were analyzed by western blotting for calnexin, TRAPα, Sec61α and L12.

B: HeLa cells were transfected for 8 days with control shRNA or the shRNA against DHHC6. On day 6 the cells were retransfected either with an empty plasmid (lanes 1&2) or with a plasmid expressing DHHC6. The cells were lysed on day 8 and immunoprecipitated using mouse anti-calnexin antibody. Immunoprecipitates were analyzed SDS-PAGE followed by western blotting

against calnexin, TRAPα, Sec61α and L12. For the analysis of the total cell lysates see Fig. S6A.

C: Western blots from (B) were quantified using Image J software and the error bars represent the standard deviation (n=3).

D: HeLa cells were transfected for 48 hrs with either WT, single or double cysteine calnexin mutants, mutant of the phosphorylation calnexin site S563A or of the TMD proline. Immunoprecipitates against anti-HA were analyzed by western blotting against: TRAPα, Sec61α, Sec62, Sec61β and L12. For the analysis of the total cell lysates see Fig. S6B.

Figure 6: Calnexin palmitoylation promotes interaction with actin

A: HeLa cells lysates were immunoprecipitated using either anti-Sec61α anti-TRAPα, anti-calnexin antibodies or no antibody. The immunoprecipitates were analyzed by western blotting against actin, calnexin and TRAPα. Blotting against Sec61α could not be performed as it migrates at the same molecular weight as the antibody heavy chain.

B: HeLa cells were transfected for 6 days with either shRNA against luciferase or shRNA against calnexin and lysed. After immunoprecipitation against Sec61α (left panel) or TRAPα (right panel), samples were analyzed by western blotting against actin, calnexin and TRAPα. As in A, Sec61α could not be probed.

C: HeLa cells were transfected with a control siRNA, siRNA against DHHC6 or DHHC3 and lysed. Immunoprecipitates against calnexin were analyzed by

Western blotting against calnexin and actin. Quantification was performed using the Typhoon Imager. Error bars correspond to standard deviations (n=4).

D: HeLa cells were transfected or not for 48h with cDNA expressing calnexin-HA WT, double or single cysteine mutants, and lysed Immunoprecipitates against HA were analyzed by western blotting against HA and actin and quantified using Typhoon Imager. Error bars correspond to standard deviations (n=4). Total cell extracts (TCE) were probed for actin.

E: HeLa cells were treated for 30 min at 37°C with either DMSO, Latrunculin A or Nocodazole or 15 min with puromycin or water, which was used as a control. The cells were lysed and immunoprecipitated with rabbit anti-calnexin antibody. The immunoprecipitates and the total cell extracts were migrated on SDS-PAGE followed by western blot to reveal calnexin, actin, TRAPα and L12 (n=3).

F: The treatment with Latrunculin A and Nocodazole was performed as in E. Immunoprecipitates against calnexin were analyzed by SDS-PAGE and followed by western blotting against calnexin, TRAPα and Sec61α. Western blots were quantified using Image J software and the error bars correspond to standard deviations (n=3).

Figure 7: Palmitoylation of Calnexin promotes the folding of glycosylated proteins

A: HeLa cells were transfected with either the control siRNA or siRNAs against DHHC6, TRAPα or DHHC3 for 72h and shRNA against calnexin for 144h. The cells were labeled with ^{35}S-Methionine/Cysteine for 20 min. The cytosolic

proteins were isolated by semi-permeabilizing the cells using digitonin. The glycoproteins were separated from the non-cytosolic fraction by using Con-A agarose beads. The glycoprotein fraction was run on SDS-PAGE and the radiolabeled products were visualized by Typhoon phosphoimager. The radiolabeled lanes were quantified using the Typhoon Imager and the histograms were plotted as the ratio of glycoproteins to the cytosolic proteins in each sample. The error bars represent the standard deviation (n=4). *** $p<0.001$. For the autoradiograms of glycoproteins and cytosolic proteins see Fig. S7A, B.

B: HeLa cells were cotransfected with either 1) control siRNA or siRNA against DHHC6 and the pSEAP2 plasmid or 2) an empty vector or the DHHC6 expressing vector and the pSEAP2 plasmid. The cell medium was replaced with fresh medium in all the plates so that the SEAP secreted in the final 24h was quantified. The SEAP secreted was normalized to the total amount of protein present in each sample and expressed as percentage of SEAP secreted by the control. * $p<0.05$.

C: HeLa cells were transfected with either the control shRNA or the shRNA against calnexin. At 96h post transfection, cells were transfected with the pSEAP2 vector and either empty vector or the vector expressing WT or mutant calnexins. At 120h post transfection, the cell medium was replaced with fresh medium in order to assess the SEAP accumulated in the last 24h. The measured SEAP values were normalized to the total amount of the protein present in each sample and the values were plotted as a percentage of the shLuc transfection. ***: $p<0.001$, ** : $p<0.01$, * : $p<0.05$.

D: HeLa cells were either cotransfected with GFP-PrP and the control siRNA or the siRNA targeting DHHC6, TRAPα. Calnexin was silenced by shRNA and GFP-PrP was transfected 96h after the shRNA transfection. Cell lysates were prepared and equal amounts of the proteins were analyzed by western blotting for GFP, calnexin, TRAPα, Sec61α, GAPDH. PrP^{p} indicates the precursor form of GFP-PrP and PrP^{m} the mature form.

E: HeLa cells were transfected with GFP-PrPwt for 24h, treated with either DMSO, Latranculin A or Nocodazole for 30 min at 37°C and prior to 30min ^{35}S-methionine-cysteine pulse labeling in the presence of the drugs. The cell lysates were immunoprecipitated with anti-GFP antibody and the immunoprecipitates were analyzed by SDS-PAGE followed by Typhoon phospho-imaging. PrP^{p} indicates the precursor and PrP^{m} the mature form of the GFP-PrP protein.

F: To monitor the binding of calnexin to the substrates HeLa cells were either treated with shRNA against DHHC6 (left panel) or shRNA against calnexin (right panel). The cells depleted of endogenous calnexin were recomplemented with either the WT or AA mutant. The cells were pulse labeled with ^{35}S-methionine-cysteine for 10 min followed by a chase of 3 min either in the presence of castanospermine or not. The lysate was immunoprecipitated using anti calnexin antibody and migrated on a SDS-PAGE followed by fixation and drying of the cells. The radiolabelled products were revealed by typhoon phosphoimager.

Figure 8: Molecular consequences of calnexin palmitoylation

When its palmitoylation sites are free, calnexin preferentially localizes to the peripheral tubular ER. Upon S-acylation by DHHC6, calnexin partitions preferentially into the rough ER and associates with TRAPα, altogether ensuring that calnexin efficiently interacts with the RTC. Once the calnexin-RTC has assembled into a supercomplex, actin is recruited and stabilizes the assembly. In this configuration, calnexin is positioned to efficiently grab nascent glycoproteins as they emerge from the translocon pore, acquire their N-linked glycan from which the 2 external glucoses have been trimmed.

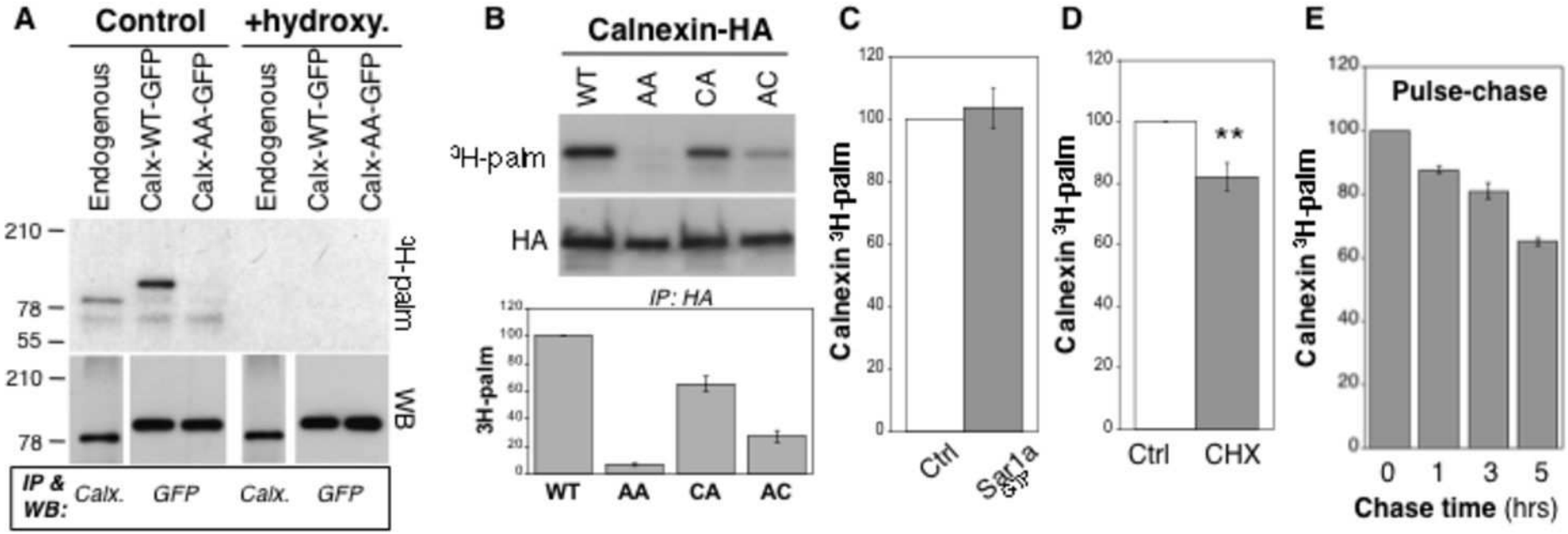
A
Control
+hydroxy.
Endogenous
Calx-WT-GFP
Calx-AA-GFP
Endogenous
Calx-WT-GFP
Calx-AA-GFP
210
78
55
210
78
3H-palm
WB
IP & WB:
Calx.
GFP
Calx.
GFP
B
Calnexin-HA
WT
AA
CA
AC
3H-palm
HA
IP: HA
3H-palm
WT
AA
CA
AC
C
Calnexin 3H-palm
Ctrl
Sar1a GTP
D
Calnexin 3H-palm
**
Ctrl
CHX
E
Pulse-chase
Calnexin 3H-palm
Chase time (hrs)

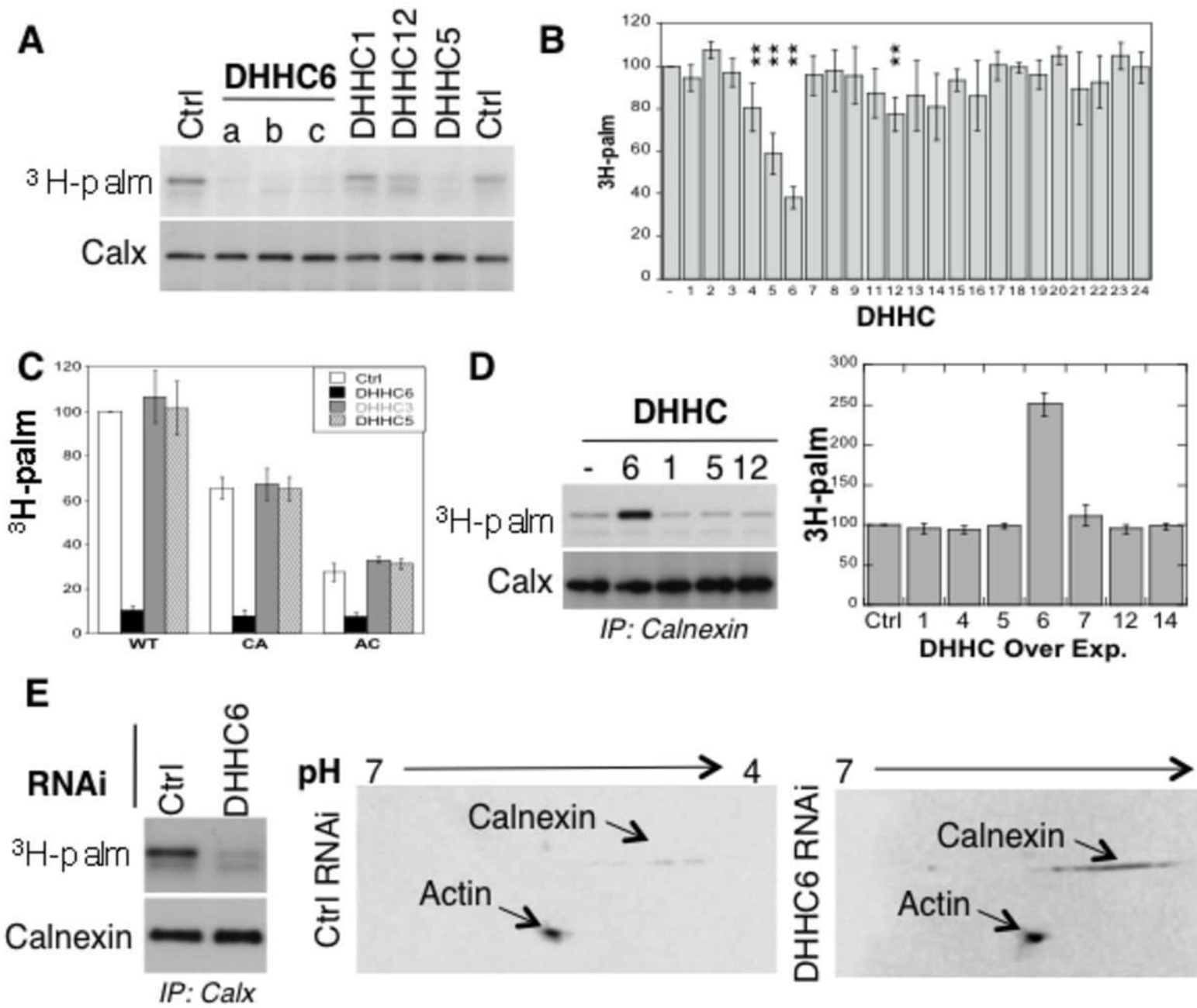
A
Ctrl
DHHC6
a
b
c
DHHC1
DHHC12
DHHC5
Ctrl
3H-palm
Calx
B
3H-palm
DHHC
C
3H-palm
Ctrl
DHHC6
DHHC3
DHHC5
WT
CA
AC
D
DHHC
- 6 1 5 12
3H-palm
Calx
IP: Calnexin
3H-palm
DHHC Over Exp.
Ctrl 1 4 5 6 7 12 14
E
RNAi
Ctrl
DHHC6
3H-palm
Calnexin
IP: Calx
pH 7 4
Ctrl RNAi
Calnexin
Actin
DHHC6 RNAi
Calnexin
Actin

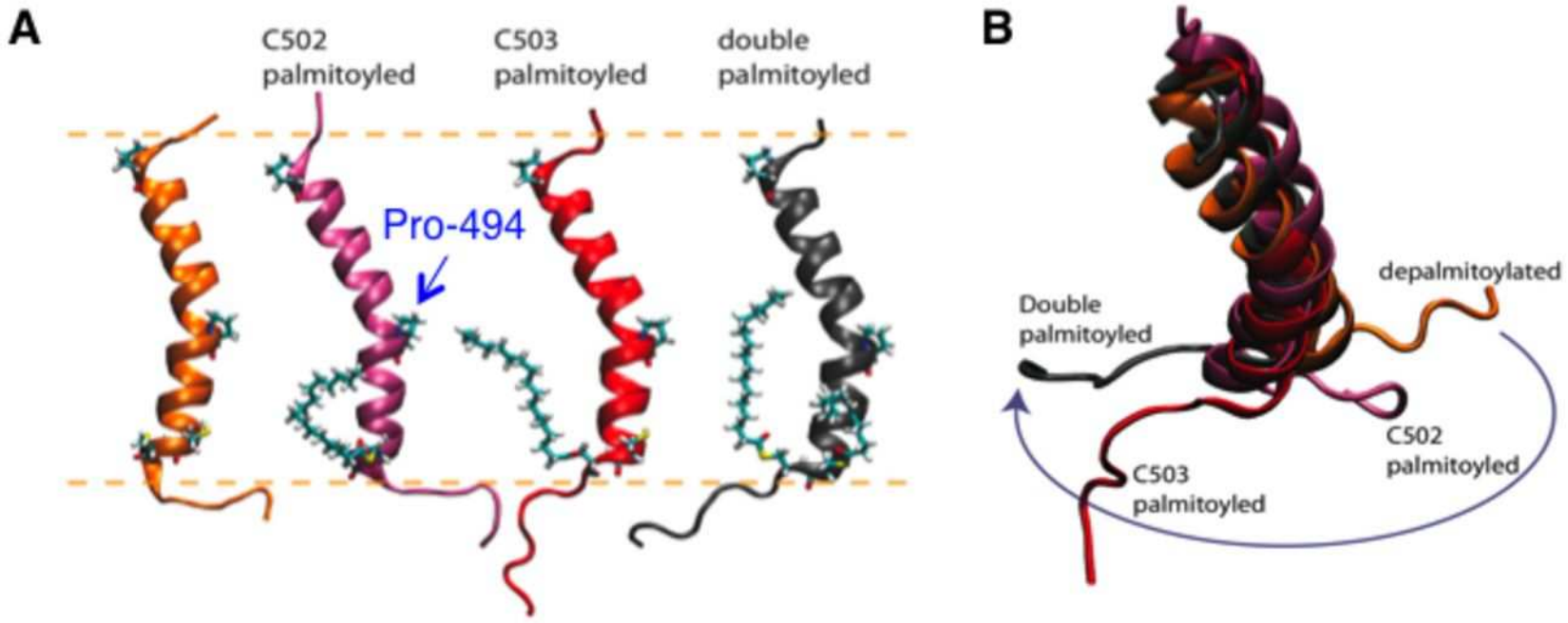
A
C502
palmitoyled
C503
palmitoyled
double
palmitoyled
Pro-494
B
depalmitoylated
Double
palmitoyled
C502
palmitoyled
C503
palmitoyled

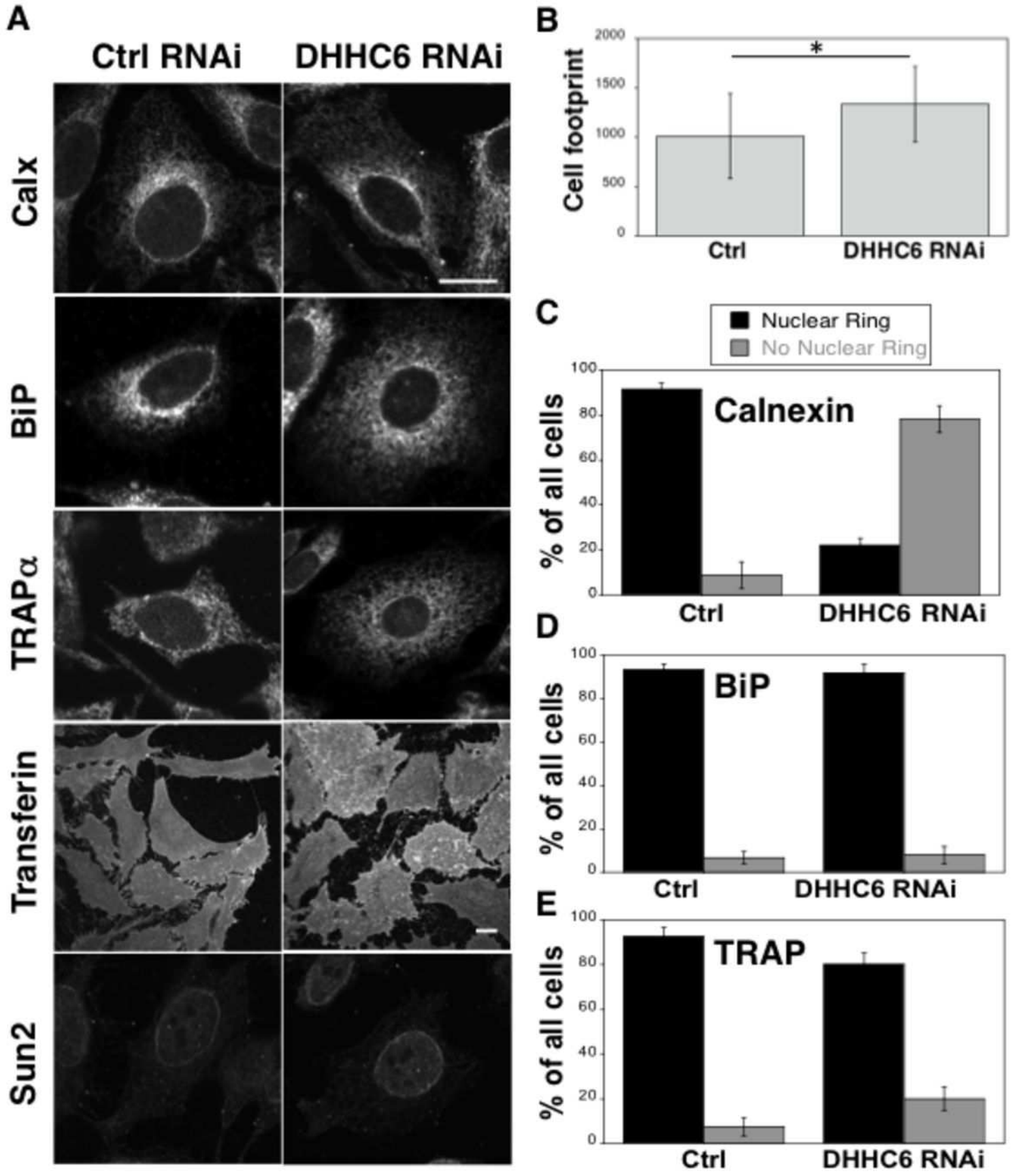
A
Ctrl RNAi
DHHC6 RNAi
Calx
BiP
TRAPα
Transferin
Sun2
B
Cell footprint
2000
1500
1000
500
0
*
Ctrl
DHHC6 RNAi
C
Nuclear Ring
No Nuclear Ring
Calnexin
% of all cells
100
80
60
40
20
0
Ctrl
DHHC6 RNAi
D
BiP
% of all cells
Ctrl
DHHC6 RNAi
E
TRAP
% of all cells
Ctrl
DHHC6 RNAi

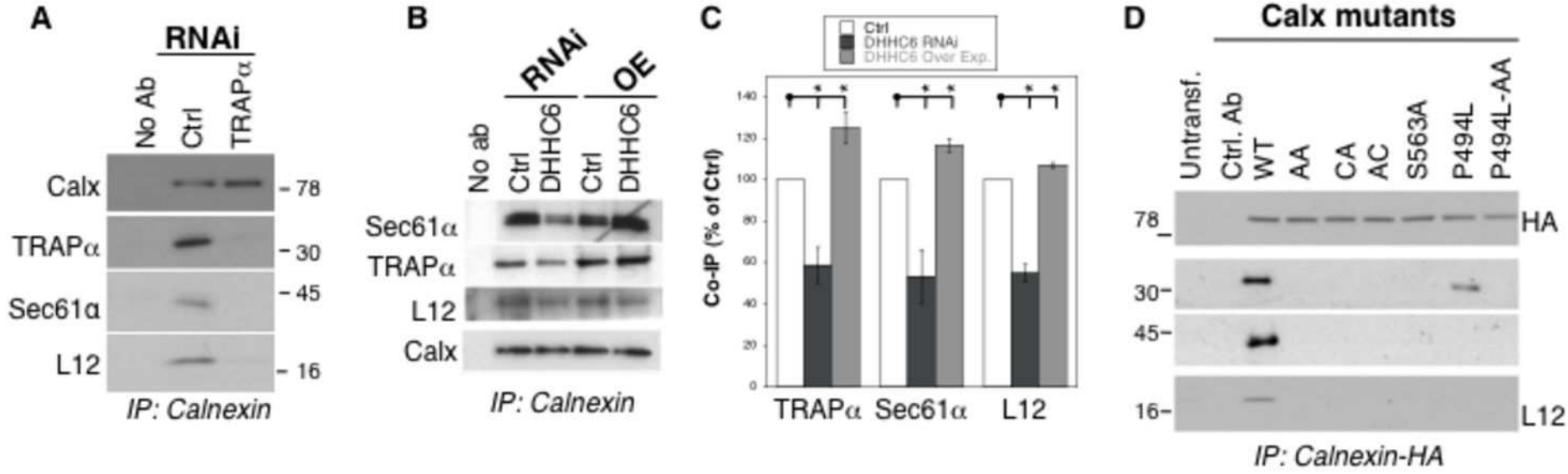
A
RNAi
No Ab
Ctrl
TRAPα
Calx
TRAPα
Sec61α
L12
78
30
45
16
IP: Calnexin
B
RNAi
OE
No ab
Ctrl
DHHC6
Ctrl
DHHC6
Sec61α
TRAPα
L12
Calx
IP: Calnexin
C
Ctrl
DHHC6 RNAi
DHHC6 Over Exp.
Co-IP (% of Ctrl)
0
20
40
60
80
100
120
140
TRAPα
Sec61α
L12
D
Calx mutants
Untransf.
Ctrl. Ab
WT
AA
CA
AC
S563A
P494L
P494L-AA
78
30
45
16
HA
L12
IP: Calnexin-HA

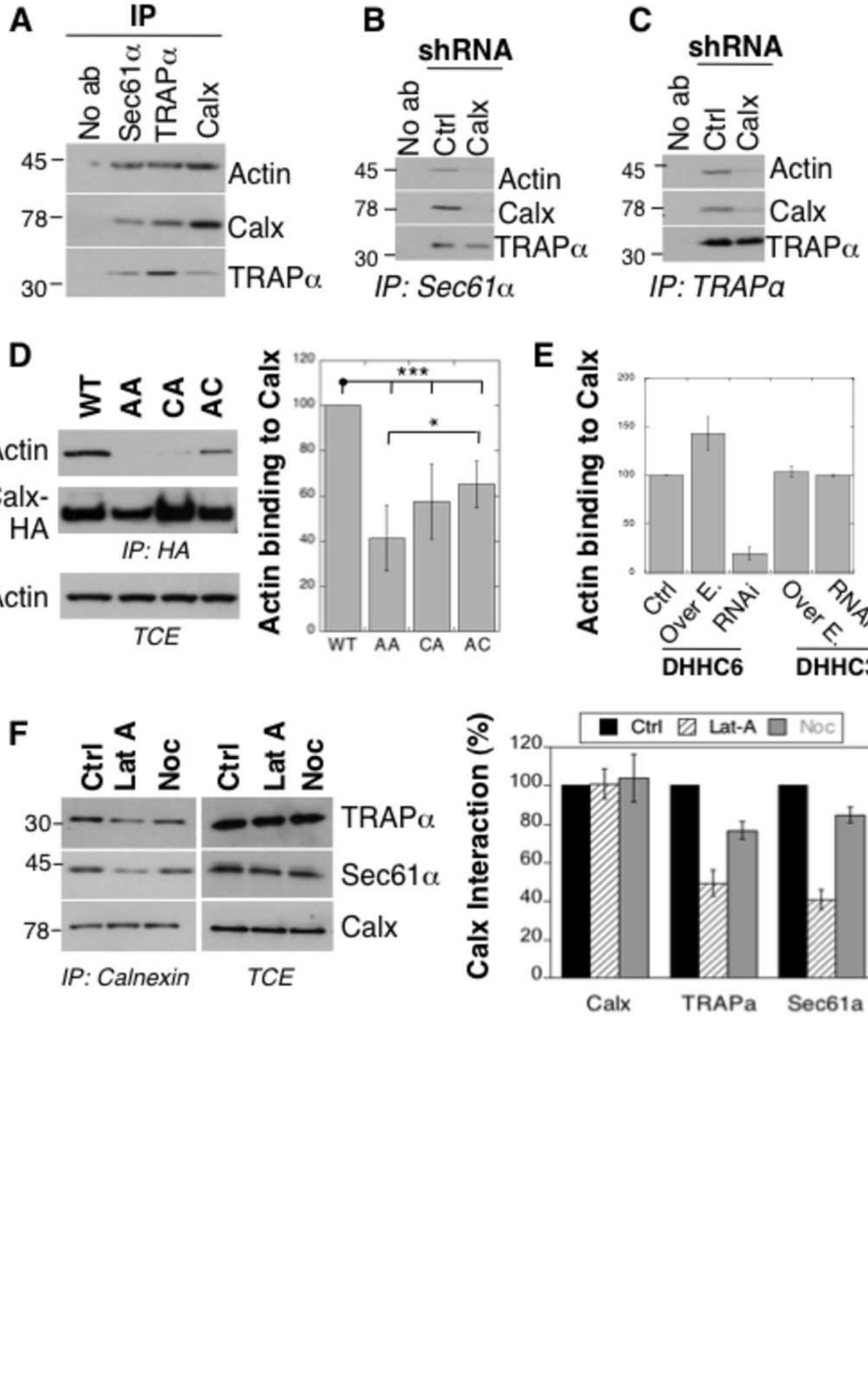
A
IP
No ab
Sec61α
TRAPα
Calx
45
78
30
Actin
Calx
TRAPα
B
shRNA
No ab
Ctrl
Calx
IP: Sec61α
C
shRNA
No ab
Ctrl
Calx
IP: TRAPα
D
WT
AA
CA
AC
Actin
Calx-HA
IP: HA
Actin
TCE
Actin binding to Calx
***
*
E
Actin binding to Calx
Ctrl
Over E.
RNAi
Over E.
RNAi
DHHC6
DHHC3
F
Ctrl
Lat A
Noc
TRAPα
Sec61α
Calx
IP: Calnexin
TCE
Calx Interaction (%)
Ctrl
Lat-A
Noc
Calx
TRAPa
Sec61a

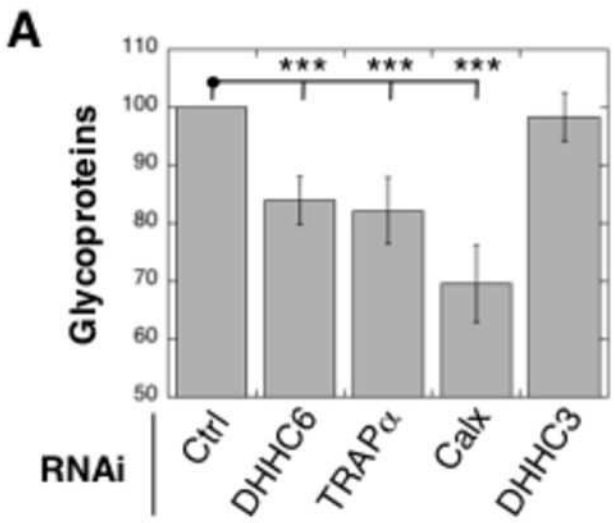
A
Glycoproteins
110
100
90
80
70
60
50
***
***
***
RNAi
Ctrl
DHHC6
TRAPα
Calx
DHHC3

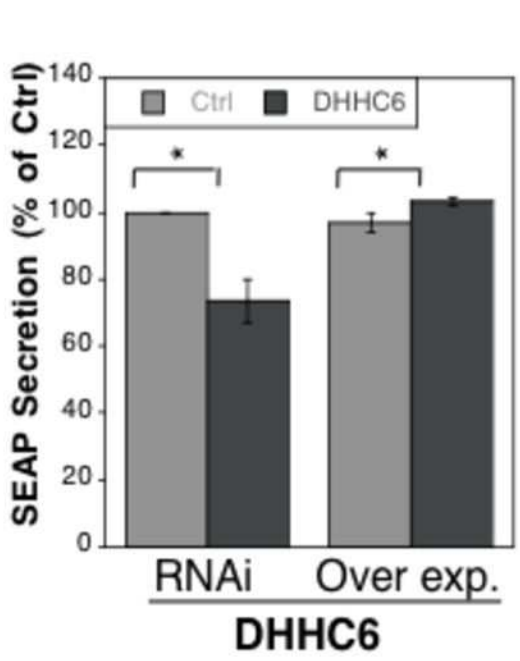
B
SEAP Secretion (% of Ctrl)
140
120
100
80
60
40
20
0
Ctrl
DHHC6
*
*
RNAi
Over exp.
DHHC6

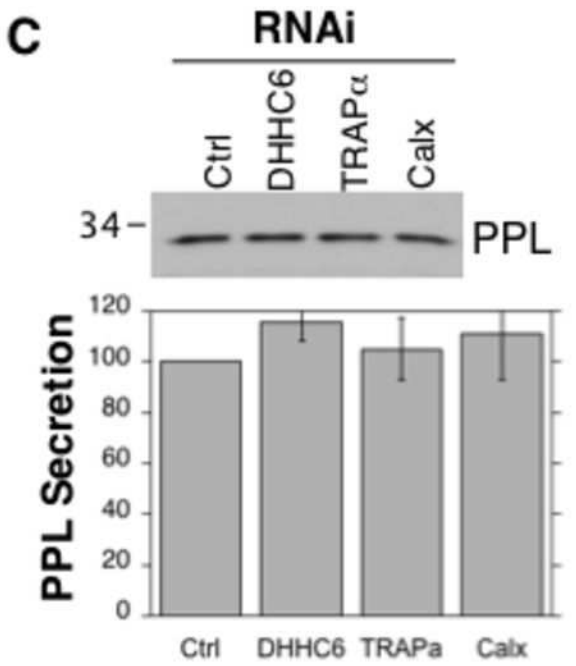
C
RNAi
Ctrl
DHHC6
TRAPα
Calx
34
PPL
PPL Secretion
120
100
80
60
40
20
0
Ctrl
DHHC6
TRAPa
Calx

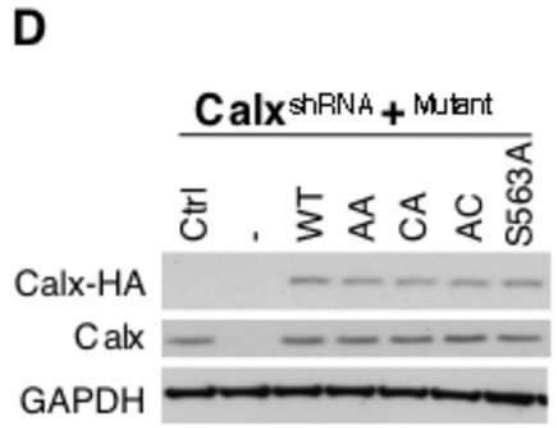
D
Calx shRNA + Mutant
Ctrl
-
WT
AA
CA
AC
S563A
Calx-HA
Calx
GAPDH

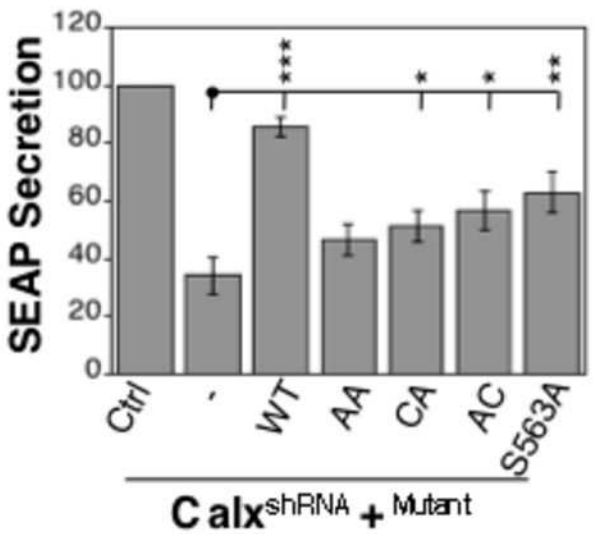
E
SEAP Secretion
120
100
80
60
40
20
0
***
*
*
**
Ctrl
-
WT
AA
CA
AC
S563A
Calx shRNA + Mutant

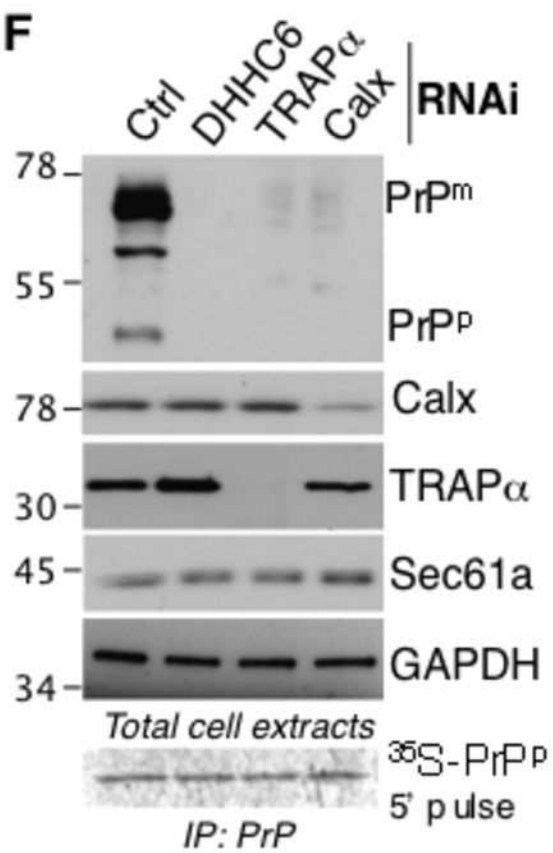
F
Ctrl
DHHC6
TRAPα
Calx
RNAi
78
55
PrPm
PrPp
78
Calx
30
TRAPα
45
Sec61a
34
GAPDH
Total cell extracts
35S-PrPp
5' pulse
IP: PrP

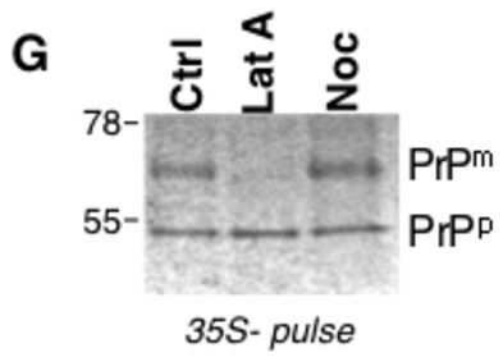
G
Ctrl
Lat A
Noc
78
55
PrPm
PrPp
35S- pulse

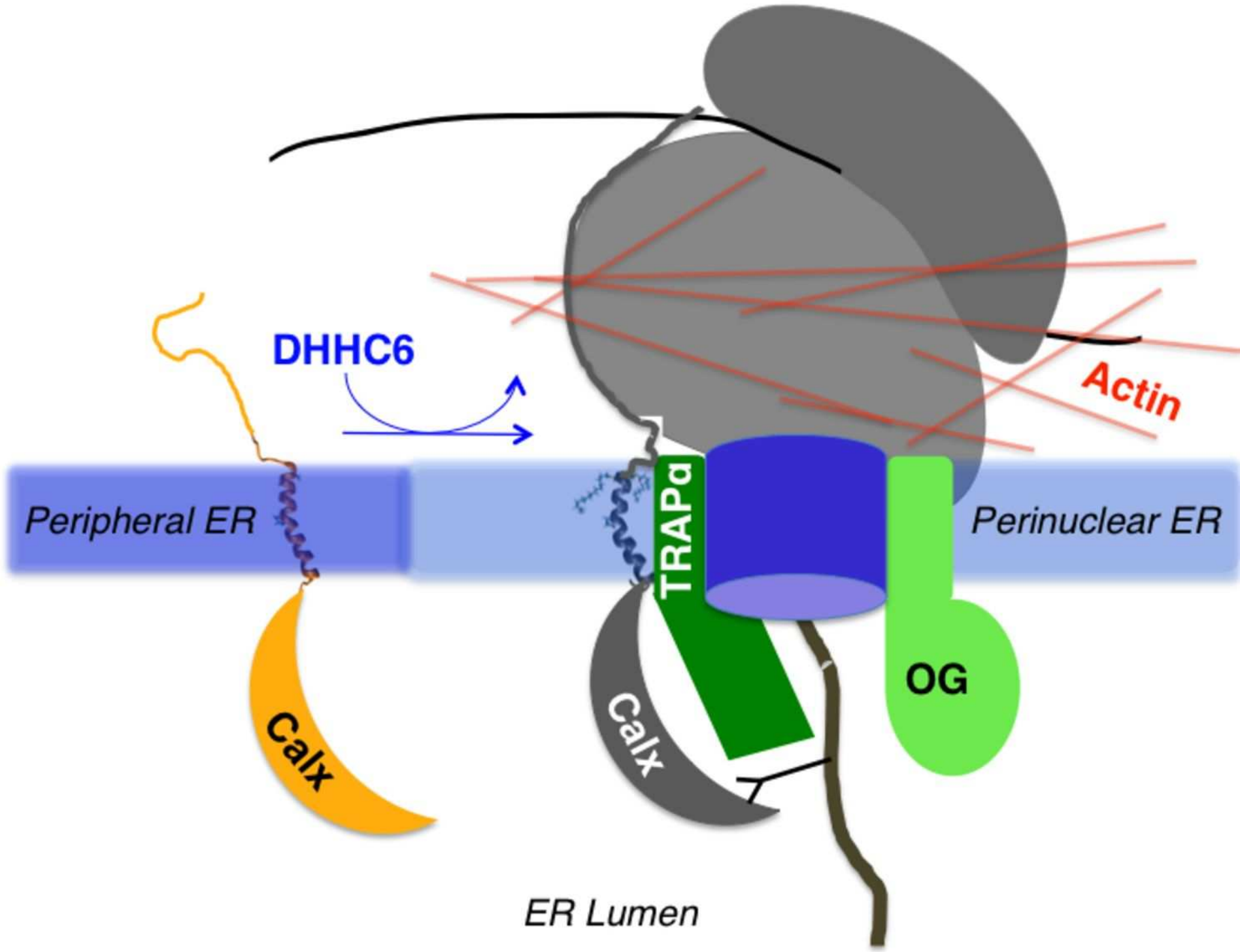
DHHC6
Actin
Peripheral ER
TRAPα
Perinuclear ER
Calx
Calx
OG
ER Lumen